



SEISMIC ANALYSIS OF THE INDIANO CABLE-STAYED BRIDGE

Paolo CLEMENTE¹, Mehmet ÇELEBI², Giovanni BONGIOVANNI¹, Dario RINALDIS¹

SUMMARY

This paper presents results of observed and analytical analyses of the dynamic response of the Indiano Cable-Stayed Bridge in Florence, Italy. The observed part is based on ambient and traffic-induced vibration tests, which allowed extracting the dynamic characteristics of the structure in terms of resonance frequencies, modal shapes and damping. These are compared with those obtained from a finite element model for which the geometrical characteristics and the mechanical properties of the materials used in the structural design of the bridge have been adopted. To supplement these analyses, equivalent static analyses were performed to yield amplitudes of response and stresses in structural elements. This version of analysis was performed by response spectrum technique using uniform response spectra expressed in terms of pseudo-velocities as input. The response spectra were obtained from contemporary, seismic hazard studies performed in Florence site.

INTRODUCTION

Identification of dynamic characteristics of structural systems is an important step that is necessary for two basic reasons:

- to assess possible dynamic behaviour of structures during strong events and
- to gain experience on the general dynamic characteristics of structural systems such that the experience and data base can be used in future design and analyses.

Past efforts in determination of dynamic characteristics of structures has facilitated development of data bases, which in turn has been used in establishing empirical formulas for estimation of fundamental periods of structures in design codes. Also, critical damping percentages used during dynamic analyses are obtained from past data bases. The data bases for dynamic characteristics of building structures are sufficiently populated. However, data on dynamic characteristics of special structures such as bridges and in particular cable-stayed bridges are scarce.

The data bases are in general obtained from two sources:

- dynamic testing of structures (forced vibration, ambient vibration, etc),
- analyses of data from instrumented structures. This however is dependent on strong-motion response data, which depends on a long duration project that is costly to implement and maintain.

¹ ENEA – Casaccia Research Centre, Rome, Italy, paolo.clemente@casaccia.enea.it

² U.S. Geological Survey, Menlo Park, CA, USA, celebi@usgs.gov

Whenever possible, low-amplitude tests are used to verify the results of analytical studies. Relevant examples of dynamic testing were carried out on recent bridges, such as the Adamillo Cable-Stayed Bridge in Sevilla [1], the Pedestrian Bridge in Burlington, Vermont [2], the Tampico Bridge in Mexico [3] and the Garigliano Bridge in Italy [4]. Wang & Huang [5] analysed the vibrations due to road roughness.



Fig. 1 Indiano Cable-Stayed Bridge, Florence, Italy

The purpose of this paper is to present observed and analytical analyses to identify the dynamic characteristics of Indiano Bridge in Florence, Italy. A general view of Indiano Bridge is shown in Figure 1. The longitudinal section, the plan view, and the cross-section with the general dimensions of the bridge are in Figure 2. The reasons for the choice of this particular bridge are:

- it is one of the longest spans in Italy,
- the structural system is simple and symmetric, thus analyses of the structural system can be performed rather reliably for comparison with measurements,
- the main span is short so that during testing extensive cabling is not necessary,
- the towers are reasonably accessible for temporary deployment of sensors.
- the bridge has a “walkway” below the deck for pedestrians and bicyclists, which facilitates deployment of sensors below the deck of the bridge rather than the top. Thus there is no interference with the flow of the traffic. And finally,
- some of the characteristics of Indiano Bridge are common to several cable bridges. For example, the presence of sliding supports at the ends causes oscillations of significant amplitude in the longitudinal direction. The deteriorated conditions of the supports also cause additional damping. These aspects make the analysis of the bridge quite complex but interesting.

DESCRIPTION OF THE STRUCTURE

The Indiano Cable-Stayed Bridge over the Arno River in Florence was completed and opened to the traffic in 1977 (Figure 1). The 189.1 m span girder of the bridge is simply supported by two piers, which are structurally independent of the other parts of the structure. In the central portion of the girder (zone M in Figure 2), whose length is 128.1 m, two boxes spaced of 6.0 m compose the cross-section. They are linked

one to another, at the upper and lower levels, by means of truss structures. As a result, the beam is characterized by large torsional stiffness. The boxes have a width of 4.0 m and a height variable from 2.6 m to 1.6 m . Cantilever beams start from the boxes to support the external portion of the road. In the zones near the ends (zones L and R in Figure 2) the cross-section becomes a three boxes cross-section.

The girder is suspended by six couples of fan-shaped stays, starting at the tops of two steel towers. Cables are regularly spread along the deck and are 3.0 m spaced from the centre line, therefore their contribution in supporting the beam torsion is very low. Six cables constrained to an external gravity anchoring compose each anchor cable.

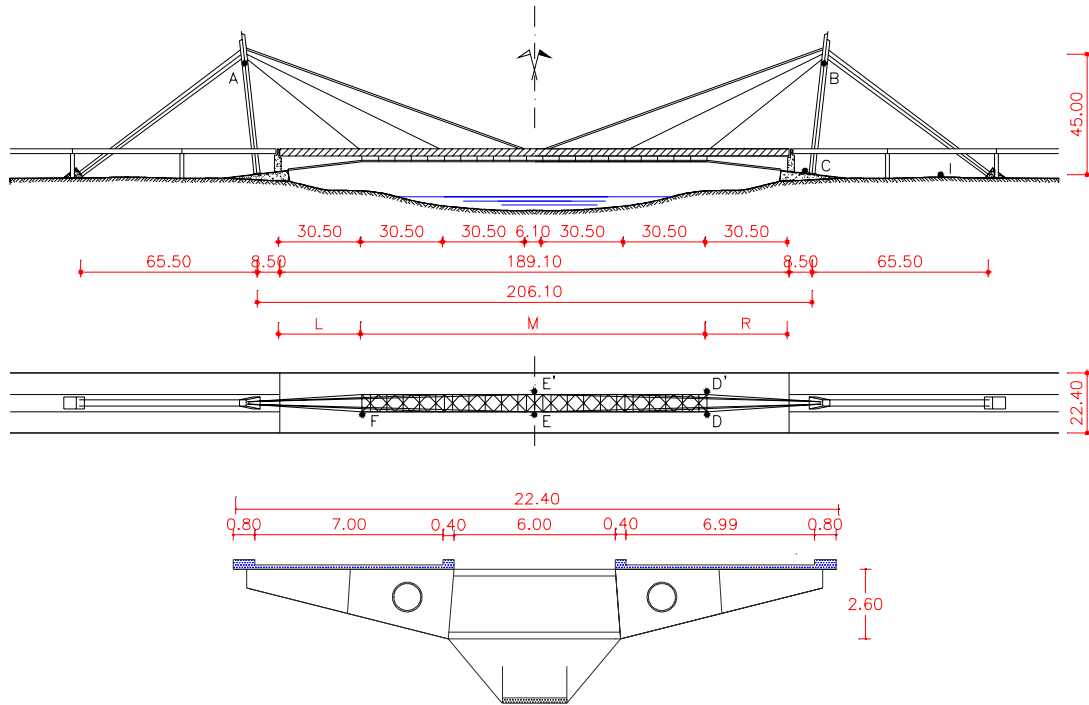


Fig. 2 General dimensions of the bridge and sensor layout (see Table 1)

The pylons have steel box cross-section and a height of about 55.0 m from the ground. They are fully constrained at their foundations, which are founded on large piles, and linked to the cable anchoring by means of a pre-stressed concrete truss, which is supposed to support the horizontal component of the tower stress. A footbridge is suspended to the girder. Due to its very high deformability, its contribution in the dynamic behaviour of the bridge is considered to be negligible. The girder is supported at each pier by means of four steel (knife-edge) roller bearings. At each bearing, lateral restraining plates stop the transversal displacements. Four pre-strained bars fixed into the pier and at the girder make the support bilateral. At the time of the experimental tests they had been considerably damaged because of the continued inversion of the reaction. As a result, the bearings were further stressed due to the uplift of the girder so much so that their sliding function was seriously compromised. This condition is believed to influence the damping characteristics of the bridge.

EXPERIMENTAL ANALYSIS

Eight Kinemetrics SS1 seismometers, an HP3566A signal conditioner and a laptop composed the experimental set-up. The synchronized signals from several seismometers were recorded by the acquisition system and analysed in real time in order to have a first glance at the experimental data.

Seismometers were temporarily installed in different locations of the structure and the free field in 11 different configurations. The various configurations of deployment of these sensors are shown in Figure 2 and are summarized in Table 1, where for each location, the directions of the sensors are indicated (x = longitudinal axis of the bridge, y = transversal axis, z = vertical axis). In configurations 9, 10 and 11, three sensors were on the ground, about 200, 100 and 50 m from the bridge, respectively. Several time-histories lasting 64 sec were recorded for each configuration to show repeatability of the vibrational characteristics and to get average values of the characteristics. In the following, each record is identified by means of the location and its direction (i.e., Ax is the sensor at A in the longitudinal direction x).

Tab. 1 Sensor locations and directions (see Figure 2)

Config.	A	B	C	D	D'	E	E'	F	Ground (distance from C)
1		$x - y$	$x - y - z$						
2	X	$x - y$	$x - y - z$						
3	x	$x - y$	$x - y - z$						
4	x	$x - y$	$x - y$	z		z		z	
5	x	$x - y$	$x - y$	y		y		y	
6	x	$x - y$	$x - y$	y		y	x		
7	x	$x - y$	$x - y$	z		z	z		
8	x	$x - y$	$x - y$	z	z	z			
9			$x - y - z$						$x - y - z$ (200 m)
10			$x - y - z$						$x - y - z$ (100 m)
11			$x - y - z$						$x - y - z$ (50 m)

Data analysis

The dynamic characteristics of the structure from analyses of observed test data are provided in terms of power spectral densities (PSD) and cross-spectral densities (CSD). Spectra were estimated by using the commercially available computer code MATLAB. Windowing was not used. In Figures 3 to 6 PSD and CSD for selected tests 10, 16 and 22, are shown. In Table 3 the resonance frequencies with the relative locations are listed. The modal shapes, obtained in the next numerical analysis, are shown in Figure 8.

The fundamental frequency, 0.61 Hz^3 , is clearly identifiable in the spectra of the records obtained at the top of the tower in the longitudinal direction (Figure 3 – Bx) and in those of the deck, both in the vertical (Figure 3 – Dz) and in the longitudinal direction ($E'z$). Ax and Bx being 180 degrees out of phase (Figure 5) and Dz , Ez and Fz in phase, the first modal shape happens to be symmetric around the mid-span. Clearly, Bx and Ez are in phase, inferring that when the towers move outwards, the deck moves upwards [Figure 11 – Mode 1].

The resonance frequency 0.81 Hz is very apparent in the spectrum of records on the deck in the longitudinal direction ($E'z$) and the cross-spectra with the records of the top of the towers confirm that

³ Just after the completion of the construction, the bridge was tested [6]. The structure was excited by dropping a suspended mass of $0.8 \text{ MNs}^2/m$ from the middle of the span. In this way only the first mode was excited. An associated frequency of 0.61 Hz was estimated.

(Figure 6 – $Bx-E'z$). The modal shape associated to this frequency consists in the longitudinal movement of tower and deck (Figure 11 – Mode 2).

Peaks at frequency 0.87 Hz identified in the spectra of the deck records in the transverse direction (Dy, Ey and Fy) indicate the fundamental transverse deck frequency. The corresponding modal shape (Figure 11 – Mode 3) represents the first mode in the transverse direction for the girder. The towers do not contribute to this mode.

Peaks at frequencies 1.04 and 1.15 Hz are apparent in the spectra of records at the tower top in the transverse direction (Figure 3 – By). The deck does not contribute to this mode. Records of sensors Ez and $E'z$, in the vertical direction during Test 25, are 180 degree out of phase at 1.15 Hz.

Peaks at frequency 1.41 Hz are apparent in the spectra of records at the tower top in the longitudinal direction (Figure 3 – Bx). Low peaks are also visible in the spectra of the vertical records on the girder (Figure 3 – Dz).

Tab. 3 Experimental resonance frequencies and estimated damping

Sensor location	Freq. (Hz)								
	0.61					1.41	1.61	2.25	
Tower longitudinal	0.61					1.41	1.61	2.25	
Tower transversal				1.04	1.15				2.61
Deck vertical	0.61			1.04	1.15	1.41	1.61	2.25	
Deck. transversal			0.87						2.61
Deck longitudinal	0.61	0.81				1.41	1.61		
Damping	6.5%	6%	4.5%	4.8%	-	-	3%	2.5%	

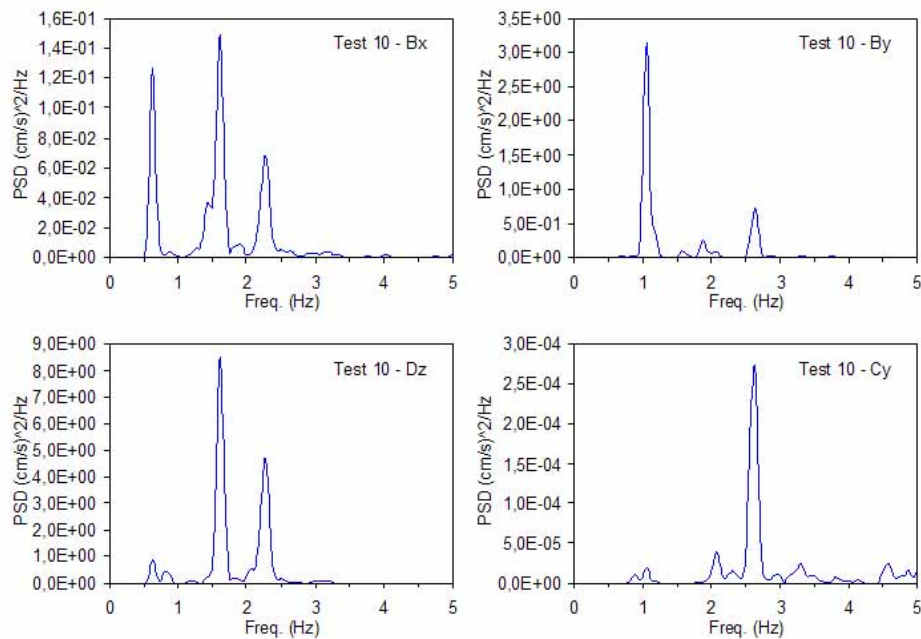


Fig. 3 Power Spectral Densities (PSD). Sensors Bx, By, Dz, Cy

At frequency 1.61 Hz, A_x and B_x (Figure 4) are 180 degrees out of phase, so they move anti-symmetrically around the mid-span. D_z and F_z are in phase at this frequency, while E_z and F_z are 180 degrees out of phase, as a result the girder shaped symmetrically with three half waves (Figure 11 – Mode 7).

At frequency 2.25 Hz A_x and B_x are in phase, D_z and F_z out of phase. A two-wave mode shape is associated with this frequency. In this case also the towers take part in the mode (Figure 11 – Mode 8). Peaks at frequency 2.61 (D_y , E_y and F_y) are relative to the second transverse mode of the girder (Figure 11 – Mode 9).

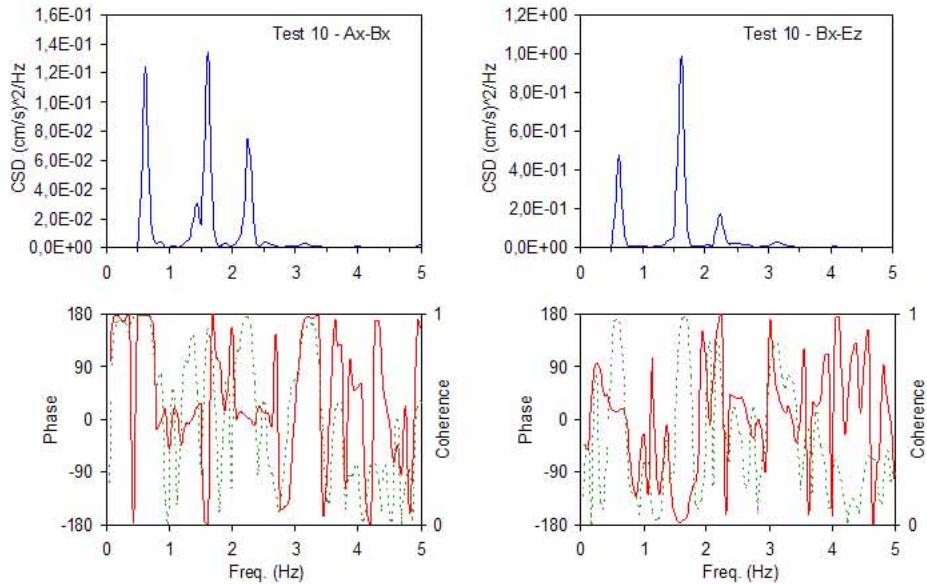


Fig. 4 Cross Spectral Densities (CSD), Phase Factor and Coherence Function (dotted line) Sensors A_x - B_x , B_x - E_z

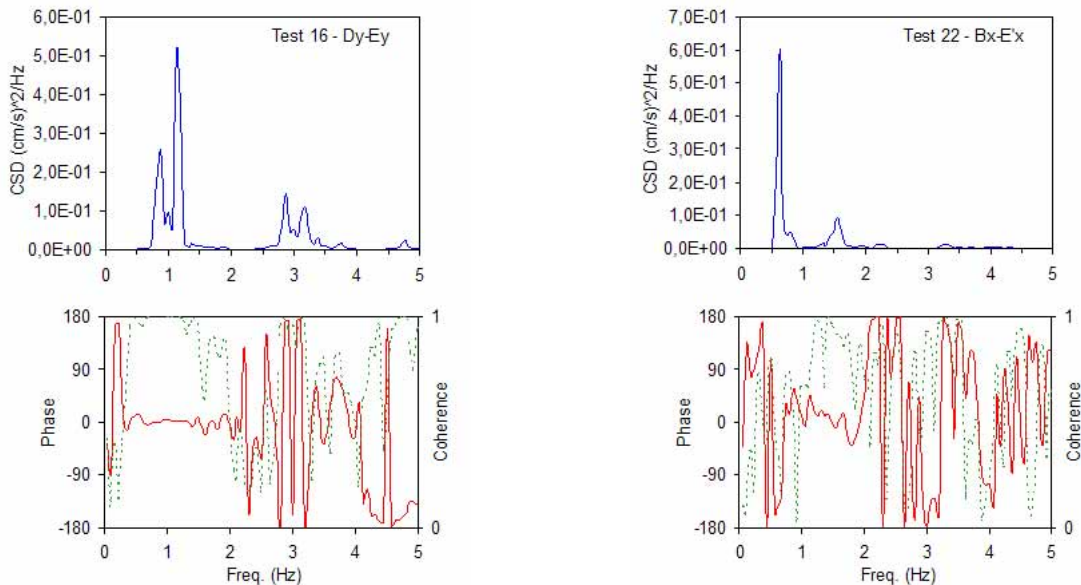


Fig. 5 CSD Sensors D_y - E_y

Fig. 6 CSD Sensors B_x - $E'x$

The critical viscous damping ratios were estimated by the half power bandwidth method and are summarized in Table 3. The values of damping obtained are very high compared with the usual ones for cable bridges. This is due to the presence of several sources of damping in joints and especially in bearings. It is restated herein that damping due to sliding supports increases for oscillation with very small amplitude [7, 8].

Consideration about site conditions

A series of noise measurements at the free field around the bridge on the north side of the river were made to assess possible effect of the site conditions on the response and behaviour of the. We kept three seismometers at the basement of one tower (location C) and moved the other three in three different positions, about 50, 100 and 200 m away from the same tower (B). For each configuration, four tests lasting 64 s were carried out. Recorded data were analysed in the frequency domain [0, 5 Hz]. Some of the natural frequencies found for the bridge appear in the ratios of PSD of horizontal to vertical components [9] at each position only for a few of the records. This is probably due to the different excitation level from the bridge traffic. A common feature for these ratios is the presence of two peaks at frequencies below 0.5 Hz.

The ratios between the PSDs of the same components at different position confirm the presence of the two peaks below 0.5 Hz. Since we are in an alluvial site these frequencies are supposed to be representative of the soil behaviour. Further investigations of the records have been excluded because this frequency value is at the limit range of the sensor response.

From this analysis we conclude that there is not any apparent relationship between the behaviour of the soil and the natural frequencies of the bridge.

MATHEMATICAL MODEL

A finite element model of the bridge was developed using the geometrical and mechanical characteristics of the bridge from the structural design drawings obtained via the Technical Office of the City Hall in Florence. The finite element computer code COSMOS (Ver. 2.5) was used for this purpose.

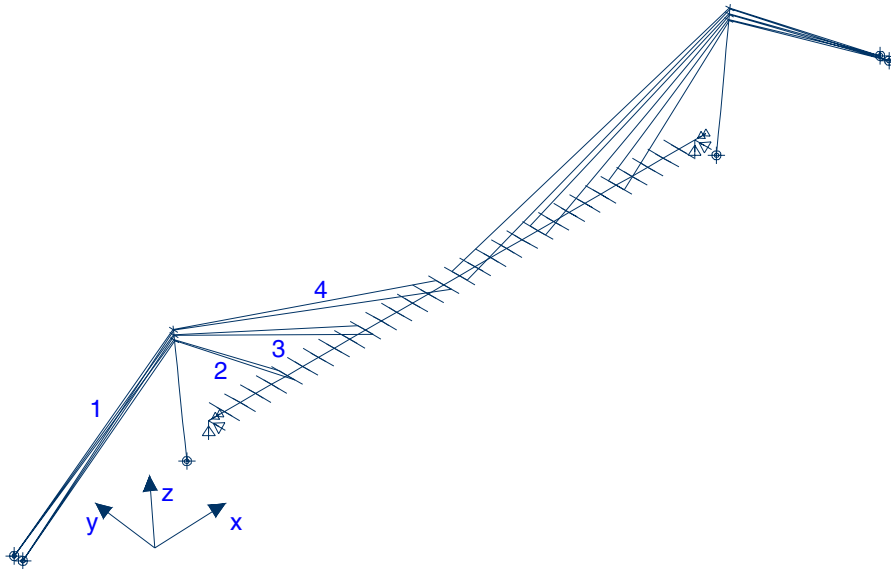


Fig. 7 Finite element model

Assumptions

The primary assumption in the finite element analysis performed is that the structure is assumed to be linear elastic. The towers are assumed to be fully constrained at their basements. The girder is simply supported at its ends; vertical displacements and torsional rotation are not allowed.

The girder and the pylons have been modelled by using 3D-beam elements. Rigid limbs have been offset both from the girder and the towers, in order to accommodate the cable attachments (Figure 7). The bending and torsional stiffness of the girder are variable along the span. In the finite element model the girder has been divided in three portions, in each of them the geometrical characteristics have been assumed to be constant and equal to the average values. These are listed in Table 4, in which A is the cross sectional area, I_y and I_z the second moments, relative to the transversal axes of the cross-section (horizontal and vertical, respectively), and J is the torsion factor. The geometrical characteristics of the towers change along their axis. These geometrical characteristics, based on design drawings as summarized in Table 5, are used to develop the mathematical model.

Tab. 4 Geometrical properties and Young's modulus of the girder beam elements

Δx	$A (m^2)$	$I_y (m^4)$	$I_z (m^4)$	$J (m^4)$	$E (MPa)$
$0 < x < 30.5 \text{ m}$	0.8637	0.7554	24.29	1.825	210000
$30.5 < x < 168.6 \text{ m}$	0.8427	0.6753	24.29	1.136	210000
$168.6 < x < 189.1 \text{ m}$	0.8637	0.7554	24.29	1.825	210000

Tab. 5 Geometrical properties and Young's modulus of the tower beam elements

Δz	$A (m^2)$	$I_y (m^4)$	$I_x (m^4)$	$J (m^4)$	$E (MPa)$
$0 < z < 12.7 \text{ m}$	0.4782	0.4453	1.075	0.8872	210000
$12.7 < z < 25.5 \text{ m}$	0.4208	0.3795	0.6373	0.6771	210000
$25.5 < z < 35.5 \text{ m}$	0.3549	0.3050	0.3557	0.4790	210000
$35.5 < z < 48.3 \text{ m}$	0.5632	0.3951	0.4615	0.6582	210000

Cables have been assumed as linear elastic truss elements. The reduction of their axial stiffness due to the sag has been accounted for by assuming reduced Young's modulus, relative to their configuration under dead loads, given by the relation ship:

$$E^* = E / \left[1 + \varphi^2 \left(\frac{1}{24} + \frac{2E}{\sigma(\varphi^2 + 24)} \right) \right]$$

Tab. 6 Cross sectional areas and apparent moduli of the cables

Cable	Number of ropes	$A (cm^2)$ (for each rope)	$E (MPa)$
1	2 * 3	119.7	200800
2	2 * 1	134.7	203300
3	2 * 1	140.5	200900
4	2 * 2	101.0	163800

where E is the Young's modulus of the cable material, σ is the stress under dead loads and $\varphi = \gamma\lambda/\sigma$ is a shape parameter, γ and λ being the weight per unit volume and the cable span, respectively [10, 11]. The cross-sectional areas and the elastic modules of the cables are provided in Table 6.

The mass of the girder ($0.140 \text{ MN s}^2/\text{m}^2$) has been increased by 10% to account for the vehicles and additional masses during the tests. The resulting distributed mass of $0.154 \text{ MN s}^2/\text{m}^2$ and the mass inertia around x-axis of $4.02 \text{ MN s}^2/\text{m}$ have been lumped at appropriate girder model nodes.

Modal Analysis

The modal analysis resulted in the frequencies listed in Table 7. The first nine modal shapes are plotted in Figure 8. The modal shapes of the numerical model and the corresponding frequencies are quite similar to the experimental ones. Discrepancies have been found only in the first resonance frequencies corresponding to the transverse and longitudinal motions of the deck. However these discrepancies can be endorsed to the differences between the actual distribution of the stiffness and the assumed ones and to the presence of unknown masses at the moment of the tests. The non-linear behaviour of the supports due to friction played an important role.

Tab. 7 Frequencies of the numerical model and experimental resonance

Mode number	Numerical Frequency (Hz)	Dominant displacements	Experimental Frequency (Hz)
1	0.61	Deck Vertical	0.61
2	0.64	Deck Longitudinal	0.81
3	0.77	Deck Transverse	0.87
4	1.12	Deck Torsion & Tower Trans.	1.04
5	1.13	Deck Torsion & Tower Trans.	1.15
6	1.37	Tower Longitudinal	1.41
7	1.62	Deck Vertical	1.61
8	2.41	Deck Vertical	2.25
9	3.09	Deck Transverse	2.61

SEISMIC RESPONSE ANALYSIS OF THE BRIDGE

Seismic Hazard Analysis

Molin and Paciello [12], using both a probabilistic approach and the analysis of a local macro-seismic catalogue, assessed the seismic hazard in Florence. Only the main points (relevant to the following spectrum response analysis) of their probabilistic approach are reported herein.

The probabilistic hazard assessment was based on the well-known Cornell's methodology [13], which models earthquake occurrences in a given time interval according to a Poisson distribution. Seismic data from GNDT (Italian National Group for Protection against Earthquakes) catalogue were used, in which only events with $M_s \geq 4.0$ or with macro-seismic intensity greater than V MCS (Mercalli-Cancani-Sieberg [14]), are reported, and the dependent events (aftershocks and foreshocks) are removed. The seismic

sources of interest for the site were selected from the seismotectonic zonation of Italian territory proposed by Scandone et al. [15]. The attenuation laws proposed by Sabetta and Pugliese [16, 17] were used for ground motion parameters.

The analysis was performed in terms of macro-seismic intensity, peak ground acceleration, peak ground velocity and pseudo-velocity response spectra. The main results can be summarized as follows. The maximum intensity historically observed in Florence is *VII* MCS. Therefore, MCS *VIII* intensity is considered as the maximum credible for the city. Thus, from these the peak ground acceleration values with 90% non-exceedence probability, in 50 and 500 years respectively, are determined as 145 and 219 cm/s^2 for shallow alluvium, and 95 and 157 cm/s^2 for deep alluvium sites. Since, the Indiano Bridge site is a deep alluvial site, in Figure 9 the uniform response spectra with 5% damping obtained for deep alluvium sites that shows the pseudovelocity values having 90% non-exceedence probability for 50, 100 and 200 years respectively are provided. The highest pseudo-velocity values are between 1 and 2 *Hz*.

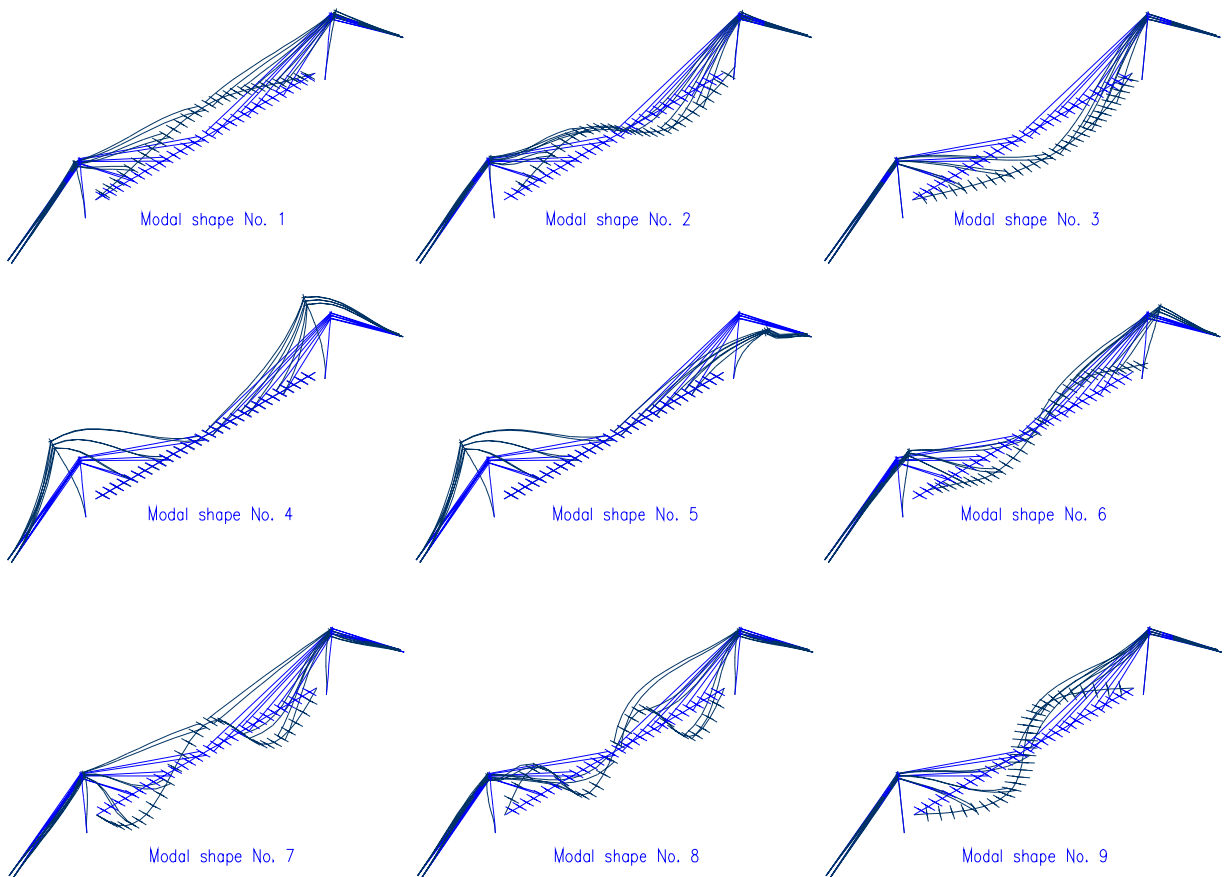


Fig. 8 Modal shapes

Response spectrum analysis

In the response spectrum analysis of the bridge, the spectrum for 5% damping and 200 years return period is used in the three main axis of the bridge, separately. The directional modal effects are considered by square root of the sum of squares of the response corresponding to directional input. Because of the structural symmetry the effects due to the input in the different directions were almost independent one of the others.

The results of the response spectrum analysis have been compared with those of the static analysis, carried out assuming the following load conditions, suggested by the Italian Code for design, construction and test of bridges [18]:

- four lanes of vehicles, two of 30.0 *KN/m* and two of 15.0 *KN/m*, symmetrically deployed with reference to the longitudinal axis of the bridge;
- a longitudinal load whose resultant is equal to 3.0 *KN/m*, simulating a braking column of vehicles;
- a transversal loads equal to 2.5 *KN/m²* acting on the bridge in presence of a vehicle column of 3.00 *m* height, simulating the wind excitation. Obviously a correct analysis of wind effects would require a more detailed study to account for the dynamic effect of the wind.

The following displacement parameters have been considered:

- maximum vertical displacement of the deck u_z , and the longitudinal displacement of the tower u_{tx} to compare with that due to load a;
- maximum longitudinal oscillation of the deck u_x , to compare with that due to load b;
- maximum transversal displacement of the beam u_y and the tower u_{ty} , to compare with those due to the wind excitation (load c).

and the following force parameters:

- maximum bending moment M_y in the beam (load a),
- maximum bending moment M_z in the beam (load c),
- maximum force in the anchor stay S_o (load a),
- maximum force in the longest stay S_m (load a),
- maximum axial force in the tower N_p (load a).

Tab. 8 Comparison between static and dynamic analysis

<i>Parameter</i>	<i>Response spectrum analysis</i>	<i>Static analysis (live loads)</i>
u_z (m)	0.100	0.469
u_x (m)	0.040	0.006
u_y (m)	0.090	0.048
u_{ty} (m)	0.074	0.026
u_{tx} (m)	0.025	0.100
M_y (MNm)	112	246
M_z (MNm)	1292	657
S_o (MN) (for each rope)	6.1	24.4
S_m (MN)	5.9	19.9
N_p (MN)	40.4	158

The results obtained are summarized in Table 8. The effects of the hypothesised earthquake are greater than those of the static analysis, especially in terms of horizontal displacements. In more detail:

- the vertical displacement of the deck and the longitudinal displacement of the tower due to static loads are lower than those due to seismic actions;
- the transversal displacement is much higher than the corresponding one due to the wind load;
- the longitudinal displacement is much higher than that due to the longitudinal force generated by a braking vehicle column;

- the value of the bending moment M_y is not negligible if compared to the moment due to static loads, while the bending moment M_z is about twice that one due to wind action;
- the axial forces in the tower and in the cables are much lower than the corresponding one due to static loadings.

CONCLUSIONS

The dynamic response assessment and consequential seismic analysis of the Indiano Cable-Stayed Bridge was performed by means of (a) observed test data and subsequent spectral analyses and (b) analytical models using design geometric parameters. Contemporarily, the study of the seismic hazard in Florence site produced the uniform response spectra in terms of pseudo-velocities. These were used as input in the dynamic analysis of the bridge, carried out in terms of response spectrum analysis.

The results can be summarized as follows:

- Several resonance frequencies are clearly identified from the observed dynamic response data and also from modal analyses using a mathematical model. The modal shapes inferred from observed data are very similar to those obtained from modal analyses using the mathematical model;
- The structure shows a modal shape whose prevalent displacements are in the longitudinal direction due to motion of the towers;
- Traffic-induced vibration amplitudes, both in vertical and in longitudinal directions, are very high, so that to determine frequent needs of maintenance works;
- Values of estimated structural damping are very high compared with those determined for cable bridges. This occurrence is related to the presence of several sources of damping (friction) in joints and in bearings;
- Even though Florence is not a high intensity seismic site, the expected earthquake based on MCS intensity VIII would cause significant increase of stresses in the bridge.

One of the characteristics of the dynamic behaviour of the Indiano Bridge is the presence of longitudinal vibrations of high amplitude. The absence of longitudinal restraints is usual in cable-stayed bridges, but in this case the above occurrence is amplified because of the absence of side cable-stayed spans and because the system is not self-anchored. From the dynamic point of view, one of the end bearings could be a fixed hinge, but the static consequences of such a kind of change should be analysed in detail (changes in the cable stresses under non-symmetrical loads, stresses in the piers due to horizontal forces).

ACKNOWLEDGEMENTS

Funding by NATO (Research Grant No. CRG 960109) is gratefully acknowledged. The authors wish also to acknowledge the Technical Office of the Florence City Hall for having allowed this study.

REFERENCES

1. Casas J. R. "Full-scale dynamic testing of the Adamillo cable-stayed bridge in Sevilla (Spain)", *Int J. Earthquake Engineering and Structural Dynamics*, John Wiley & Sons, 1995; 24(1): 35-51.
2. Gardner-Morse M.G. & Huston D.R. "Modal Identification of Cable-Stayed Pedestrian Bridge", *Journal of Structural Engineering*, ASCE, 1993; 119(11): 3384-3404.
3. Murià-Vila D., Gomez R & King C. "Dynamic Structural Properties of Cable-Stayed Tampico Bridge", *Journal of Structural Engineering*, ASCE, 1991; 117(11): 3396-3416.
4. Clemente P., Marulo S., Lecce L. & Bifulco A. "Experimental modal analysis of the Garigliano cable-stayed bridge", *Int. J. Soil Dynamics and Earthquake Engineering*, Elsevier Science, 1998; 17(7-8): 485-493.

5. Wang T.L. & Huang D. "Cable-Stayed Bridge Vibration due to Road Surface Roughness", *Journal of Structural Engineering*, ASCE, 1992; 118(5): 1354-1374.
6. Augusti G., Chiarugi A., Vignoli A. "Analisi sperimentale di un ponte strallato", *Proc. 7th Italian Conference on Steel Structures* (Torino 1979), C.T.A. Milano, 1979 (in Italian).
7. Kawashima K. & Unjoh S. "Damping Characteristics of Cable-Stayed Bridges Associated with Energy Dissipation at Movable Bearings", *Proc., Japan Society of Structural Engineering and Earthquake Engineering*, 1989; No. 404, 6(1): 145-152.
8. Kawashima K., Unjoh S. & Tunomoto M. "Estimation of Damping Ratio of Cable-Stayed Bridges for Seismic Design", *Journal of Structural Engineering*, ASCE, 1993; 119(4): 1015-1031.
9. Nakamura Y., "A method for Dynamic Characteristics estimation of Subsurface using Microtremor on the Ground Surface", *QR of RTRI*, 1989; 30(1): 25-33.
10. Clemente P., D'Apuzzo M. "Analisi del modello generalizzato di ponte strallato" *Fondazione Politecnica per il Mezzogiorno d'Italia*, Giannini Napoli, 1990; No. 162 (in Italian).
11. D'Apuzzo M., Clemente P. "Progetto preliminare dei ponti strallati", *Autostrade*, Autostrade-Italstat Roma, 1990; 3: 70-78 (in Italian).
12. Molin D. & Paciello A. "Seismic Hazard Assessment in Florence City Italy", *Journal of Earthquake Engineering*, Imperial College Press, 1999; 3(4): 475-494.
13. Cornell C. A. "Engineering seismic risk analysis", *Bull. Seism Soc. Am.*, 1968; 58(5): 1583-1606.
14. "MCS, Mercalli-Cancani-Sieberg macroseismic scale", From Sieberg A., *Geologie der Erdbeben, Handbuch der Geophysic*, Tab. 2 and 3, Berlin, 1930.
15. Scandone P., Patacca E., Meletti C., Bellatalla M., Perilli N. & Santini U. "Struttura geologica, evoluzione cinematica e schema sismotettonico della penisola italiana", *Atti Convegno GNDT* (Pisa, 1990), GNDT, 1991; 1.
16. Sabetta F. & Pugliese A. "Attenuation of peak horizontal acceleration and velocity from Italian strong-motion records", *Bull. Seism. Soc. Am.*, 1987; 77(5): 1491-1513.
17. Pugliese A. & Sabetta F. "Stima degli spettri di risposta da registrazioni di forti terremoti italiani", *Ingegneria Sismica*, 1989; 2: 3-14 (in Italian).
18. Ministero Lavori Pubblici "Aggiornamento delle norme tecniche per la progettazione, l'esecuzione e il collaudo dei ponti stradali - D.M. LL.PP. 4 maggio 1990", *G.U. Repubblica Italiana*, 29 Jan. 1991.